Journal of Neuroscience Methods 204 (2012) 159–167

Contents lists available at SciVerse ScienceDirect

Journal of Neuroscience Methods

journal homepage: www.elsevier.com/locate/jneumeth

Basic Neuroscience

Extraocular muscle motor units characterized by spike-triggered averaging in alert monkey

Paul D. Gamlin[a,*], Joel M. Miller[b,c]

[a] Department of Vision Sciences, University of Alabama at Birmingham, AL, United States
[b] Eidactics, San Francisco, CA, United States
[c] Smith-Kettlewell Eye Research Institute, San Francisco, CA, United States

ARTICLE INFO

Article history:
Received 4 October 2011
Received in revised form 8 November 2011
Accepted 8 November 2011

Keywords:
Medial rectus
Motor unit
Muscle force transducer
Recruitment
Spike-triggered averaging

ABSTRACT

Single-unit recording in macaque monkeys has been widely used to study extraocular motoneuron behavior during eye movements. However, primate extraocular motor units have only been studied using electrical stimulation in anesthetized animals. To study motor units in alert, behaving macaques, we combined chronic muscle force transducer (MFT) and single-unit extracellular motoneuron recordings. During steady fixation with low motoneuron firing rates, we used motoneuron spike-triggered averaging of MFT signals (STA-MFT) to extract individual motor unit twitches, thereby characterizing each motor unit in terms of twitch force and dynamics. It is then possible, as in conventional studies, to determine motoneuron activity during eye movements, but now with knowledge of underlying motor unit characteristics.

We demonstrate the STA-MFT technique for medial rectus motor units. Recordings from 33 medial rectus motoneurons in three animals identified 20 motor units, which had peak twitch tensions of 0.5–5.25 mg, initial twitch delays averaging 2.4 ms, and time to peak contraction averaging 9.3 ms. These twitch tensions are consistent with those reported in unanesthetized rabbits, and with estimates of the total number of medial rectus motoneurons and twitch tension generated by whole-nerve stimulation in monkey, but are substantially lower than those reported for lateral rectus motor units in anesthetized squirrel monkey. Motor units were recruited in order of twitch tension magnitude with stronger motor units reaching threshold further in the muscle's ON-direction, showing that, as in other skeletal muscles, medial rectus motor units are recruited according to the "size principle".

1. Introduction

Morphological and histochemical studies conventionally distinguish six types of extraocular muscle fibers based on fatigability, laminar location, and whether they produce twitches or graded contractions (Alvarado and Van Horn, 1975; Peachey et al., 1974; Spencer and Porter, 1988). Given these multidimensional specialized characteristics, and the likelihood that all fibers driven by a given motoneuron are of the same type (Porter et al., 1995), one would expect there to be similarly distinguishable types of motor units (a motoneuron and the set of muscle fibers it innervates). Determining motor unit type, however, requires measurement of the magnitude and temporal profile of forces produced by its muscle fibers, as well as motoneuron activity, which until now has only been possible using electrical stimulation in anesthetized animals (e.g. Shall and Goldberg, 1992). These studies support the notion of physiological heterogeneity of extraocular motor units in both cats and monkeys (e.g. Shall and Goldberg, 1992; Goldberg and Shall, 1999), but electrophysiological studies in alert macaques nevertheless continue to consider motoneurons as a single functional class, differing only on continua of threshold and sensitivity (e.g. Fuchs and Luschei, 1971; Robinson, 1970; Fuchs et al., 1988; Gamlin et al., 1989; Gamlin and Mays, 1992; Sylvestre and Cullen, 1999). Thus, to date, electrophysiological study of oculomotility in alert macaques has been limited to correlating motoneuron activity with eye movement, without regard to motor unit type.

In other motor systems, motor units are characterized by averaging muscle force measurements triggered on electromyographic activity (e.g. Cheney, 1980; Thomas et al., 1986), motoneuron spikes (e.g. Lemon, 1993), or motoneuron axon stimulation (e.g. Westling et al., 1990; Macefield et al., 1996). We recently developed a new generation of chronically implantable muscle force transducer (MFT) that is able to measure total physiological oculorotary extraocular muscle tension in alert, behaving animals for several months (Miller et al., 2011). In the study reported here we characterized medial rectus motor units in alert, behaving

* Corresponding author at: 636A Worrell Building, University of Alabama at Birmingham, Birmingham, AL 35294, United States. Tel.: +1 205 934 0322; fax: +1 205 934 5725.
E-mail address: pgamlin@uab.edu (P.D. Gamlin).

0165-0270/$ – see front matter © 2011 Elsevier B.V. All rights reserved.
doi:10.1016/j.jneumeth.2011.11.012

macaques by simultaneously measuring medial rectus muscle force and motoneuron activity, and using motoneuron spike-triggered averaging of MFT signals (STA-MFT) to extract individual motor unit twitches.

Motor unit twitch responses are best characterized at low motoneuron firing rates (10–30 Hz) where temporal overlap of twitches is minimal, and likely nonlinear summation does not distort individual twitch profiles. Subsequently, determining the participation of the motor unit in other eye movement regimens, involving higher or rapidly changing firing rates, is then straightforward. Specifically, since the motor unit twitch has already been characterized at a low firing rate, it is not essential to attempt STA twitch extraction during those eye movements in which motoneuron firing rate is high or rapidly changing.

We measured twitch tensions consistent with those reported in unanesthetized rabbits (Barmack, 1977), and with estimates of the total number of medial rectus motoneurons and rectus muscle twitch tension generated by whole-nerve stimulation in monkey (Fuchs and Luschei, 1971), but substantially lower than those reported for motor units in anesthetized squirrel monkey (e.g. Shall and Goldberg, 1992; Goldberg and Shall, 1999). Motor units were recruited in order of twitch tension magnitude, with stronger motor units reaching threshold further in the muscle's ON-direction, showing that, as in other skeletal muscles, medial rectus motor units are recruited according to the "size principle".

2. Materials and methods

2.1. Muscle force measurement

MR muscle forces were measured with strain gauge based muscle force transducers (MFTs) of our design (Miller et al., 2011), earlier versions of which have been described elsewhere (Miller et al., 2002; Miller and Robins, 1992). Larger and less refined versions of such "buckle" force transducers have previously been implanted on the tendons of hindlimb muscles in cats to measure force generation (e.g. Walmsley et al., 1978) and motor units properties (e.g. O'Donovan et al., 1983). Our MFTs measure *total oculorotary force*, delivered by the muscle at its insertion into the globe, summed across the width of the muscle. With the eye allowed to rotate normally, they measure neither isometric nor isotonic force, but *physiologic force*, the force determined by the relationship between innervation and muscle stretch that obtains as the eye rotates normally in an alert behaving subject. Each MFT was calibrated by attaching it to a strain gauge amplifier (Vishay Micro-Measurements Model 2311, Raleigh, NC) with 2 V excitation, inserting a pin through its bearings, threading a length of 1/8″ wide Mylar tape through it as the muscle would go, and hanging weights 5–80 g from the end of the tape. All functioning devices have similar sensitivities, no measurable hysteresis, and are almost perfectly linear (Miller et al., 2011). MFT implantation does not require disinserting the muscle or disturbing connective tissues deeper than about 10 mm behind the insertion. The devices are small, and protrude little from the muscles they are attached to. MFT frames conform to the shape of the globe and are unlikely to become unloaded when the muscle wraps around the globe in contralateral gaze. It is possible to imagine surrounding tissues exerting changing pressures on an MFT or restricting eye rotation, but we have shown that any such forces are insufficient to produce detectable binocular misalignment within a ±20° field with the eyes visually dissociated (that is, when binocular motor fusion could not mask a mechanical imbalance), and that effects on saccade dynamics are modest (10% decrease in peak saccadic velocity; Miller et al., 2002). The two parallel beams to which strain gauges are bonded are each 1 mm wide by 0.25 mm thick half-hard stainless steel, which is much stiffer than the connective tissue that grows to envelop the implanted device, so that device sensitivity is unlikely to be measurably affected by scarring. A successfully implanted MFT is stable for several months or longer. An outline of MFT fabrication is given in Appendix A. Complete fabrication instructions may be found at "eidactics.com/Eidactics-branch/Products/MFT/MFT-Fabrication.pdf".

2.2. Animal preparation

Three male, adult rhesus monkeys (*Macaca mulatta*), M1, M2, and M3, were used in these studies, which were approved by the Institutional Animal Care and Use Committees of The Smith-Kettlewell Eye Research Institute and the University of Alabama at Birmingham, and followed the Guide for the Care and Use of Laboratory Animals (National Research Council, 1996). Surgery was performed under aseptic conditions. General anesthesia was induced with ketamine and maintained with isoflurane. Analgesics and antibiotics were administered postsurgically, as prescribed by attending veterinarians.

A scleral search coil (Robinson, 1963) was implanted on one eye of each *M. mulatta* using the method of Judge et al. (1980), except that we sutured the coil to the sclera, using either 7-0 Dacron or 6-0 Vicryl on a spatula needle, to prevent slip. We trained the monkey to fixate targets and perform eye movements for juice reward, and then implanted a recording cylinder on each side of the skull, over the midbrain at a 15° angle to the sagittal plane. Once medial rectus notoneurons had been localized, we implanted a second eye coil and MFTs on the horizontal muscles of one eye.

MFTs were implanted as follows. We disinserted the conjunctiva at the limbus in quadrants containing muscles to be implanted, and placed traction sutures in cut conjunctival edges to aid in visualizing muscles. We cleared each muscle of attachments by blunt dissection to about 10 mm posterior to its insertion, and placed it on a special tendon lifter (Fig. 1B).

MFTs are fabricated in mirror-image configurations, and one was chosen such that its lead wires would project posteriorly and superiorly. Holding it in its forceps (Fig. 1A), we passed the tendon lifter, with the tendon on it, up through the MFT's aperture. Pulling the muscle gently upward, while holding the MFT down against the globe, we pushed a fitted pin through the proximal bearings, under the muscle, and through the distal bearings. With the MFT positioned a few mm behind the insertion, and oriented squarely on the muscle, we passed a 6-0 Prolene suture on a round, non-cutting needle through each tie-down hole and secured it to the underlying muscle margin; it is important to stabilize the MFT until it becomes enveloped with connective tissue, or it is likely to rotate on the muscle, delivering a signal reduced by the cosine of the angle of rotation. We positioned the lead wire in the orbit, allowing some slack, and routed it to the scalp, following the method used to implant eye coil wires (Judge et al., 1980) (Fig. 1C).

Because strain gauge signals are small resistance changes, electrical connections must be scrupulously maintained. The braided MFT lead wires were passed uninterrupted into a special plastic Connector Can, where they were soldered to easily cleaned pins, onto which strain gauge amplifier connections were made for data collection (Fig. 1C).

MFT signals were read with a DC strain gauge amplifier (Vishay Micro-Measurements Model 2120B or Model 2311, Raleigh, NC). Previous studies (Miller et al., 2002) have shown that MFT gains are stable from implantation to excision, unless moisture intrusion has caused the device to fail. Thus we assume that gains measured prior to implantation are valid during implantation.

For spike-triggered averaging, the signal from the strain gauge amplifier was further amplified 100× (2 Hz–1 kHz band pass) by an AC differential amplifier (Bak Electronics) and recorded.

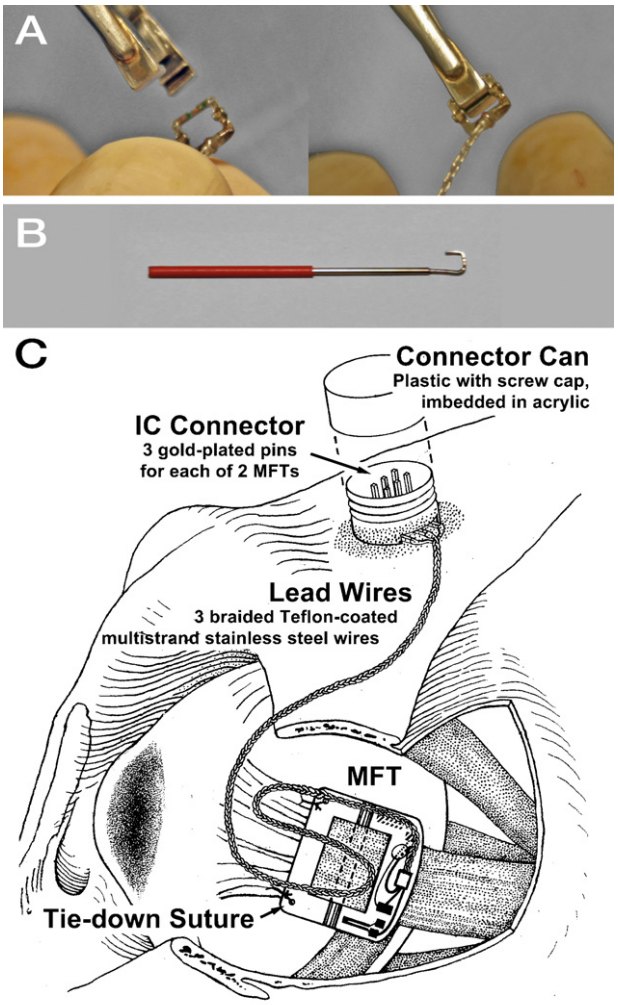

Fig. 1. MFT Installation. (A) MFT forceps are custom-made locking forceps with tips designed to designed to fit and hold an MFT securely, without damaging its coatings. (B) MFT Tendon Lifters are small muscle hooks with handles and hooks able to pass up through the MFT's aperture. (C) MFT installation on monkey lateral rectus muscle: The muscle is directed through the MFT by a pin inserted through the device's bearings and under the muscle. Non-absorbable tie-down sutures stabilize the devices orientation. Implantation does not require disinserting the muscle.

2.3. Eye movement recording

At the beginning of each recording session, horizontal and vertical gains of each eye were calibrated independently. This was done by having the animal monocularly fixate targets at various horizontal and vertical positions. Animals showed little variability in fixation from trial to trial and saccades of <0.2° could be reliably detected. The positions of both right and left eyes were sampled at 1 kHz and stored for later analysis.

2.4. Other instrumentation

For monkey M1, LED visual targets at 100 cm distance were controlled, binocular eye position monitored and recorded, juice reward dispensed, and motoneuron firing recorded with a PXI-based LabOS^{TM} data acquisition and control system (see "eidactics.com/Common_Pages/Projects/LabOS"). For monkey M2, the visual display was a dual-channel optical stimulator with a field of view of ±18° (Gamlin and Yoon, 2000; Zhang and Gamlin, 1998). For monkey M3, the display was a 90° × 70° rear-projection screen at 95 cm illuminated by an Electrohome Marquee 8500 projector at 1600 × 1200 resolution. To elicit symmetric and asymmetric vergence eye movements, a pen plotter under computer control was used to move an LED visual target in depth and horizontally.

2.5. Motoneuron recording

Using a Kopf microdrive, a Parylene-insulated tungsten microelectrode mounted in a 26-ga cannula was advanced through a 21-ga hypodermic syringe puncturing the dura. Unit activity was sharply filtered above 5 kHz, and spikes were detected with a window discriminator and recorded digitally to computer to the nearest 0.1 ms. The recording electrode (0.3–0.6 MΩ) was lowered to the medial rectus subdivision of the oculomotor nucleus. Criteria for localizing neurons within the medial rectus subdivision have previously been described (Gamlin and Mays, 1992), and on this basis, cells selected for this study all appeared to be in the medial rectus subdivisions of the oculomotor nucleus. Once the activity of an individual medial rectus motoneuron was sufficiently isolated to permit single-unit recording, trials of 8–25 s were run sequentially. During these trials, the animal fixated a target along the horizontal meridian at the position that resulted in firing rates of 10–30 spikes/s.

2.6. Data analyses

The stored data were analyzed off-line using Linux and Apple computers with custom interactive software.

2.7. Spike-triggered averaging of MFT signals

Amplified MFT signals saturated briefly after saccadic eye movements (Fig. 2A) and made large excursions after microsaccades and blinks so, prior to averaging, we manually selected for analysis those periods of the trials that were relatively unaffected by eye movement-related artifacts. For each motoneuron action potential (spike) within these periods of steady fixation, the computer generated a 60 ms averaging window (from 10 ms before to 50 ms after) on the amplified MFT trace at 1 ms resolution. For each extracted twitch, we averaged data from 1000 to 6000 action potentials. For each time point, we calculated the mean and standard deviation (SD) of the averaged value, and calculated 95% confidence limits as (SD*1.96)/(square root (number of spikes)). We plotted the mean and 95% confidence limits against time.

2.8. Single-unit firing rate/eye position analysis

Initially, we computed firing rate-eye position slopes for various conjugate eye positions. Eye position and unit activity were displayed, and periods of steady fixation were manually delineated. Averages of horizontal and vertical positions of left and right eyes, and average firing rates were computed for successive 100 ms samples over these periods. Cells were recorded from both sides of the brain, and firing rate-eye position relationships are reported with reference to the ON-direction of the recorded motoneuron population (positive thresholds correspond to eye positions in the ON-direction, and positive slopes to increased firing in the ON-direction). A scatter plot was generated for each cell, and correlation coefficients and linear regression parameters were calculated. The firing rate of the cell was plotted as a function of conjugate eye position. This yielded a measure of the position sensitivity of the cell for conjugate eye movements (k_C). Extrapolation of this slope to zero firing rate estimated the threshold (T) for the cell, with negative values in the OFF-direction.

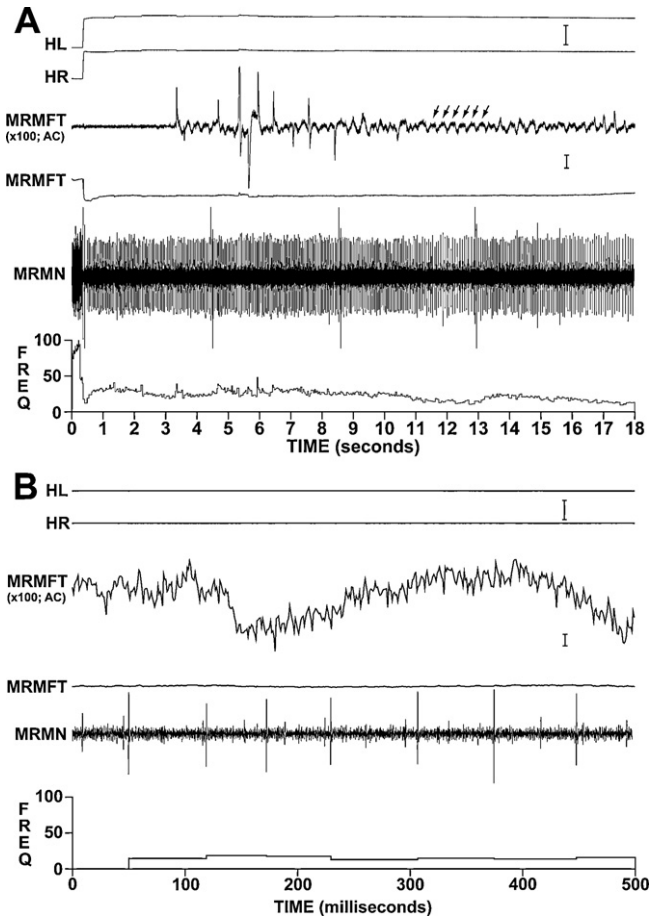

Fig. 2. Raw Data. (A) 18-s recording of single-unit activity of a right medial rectus motoneuron and force from an MFT on the right medial rectus muscle (MRMFT). Upper scale bar = 10°; lower scale bar = 2 g (MRMFT) and 40 mg (MRMFT, 100×; AC). Arrows indicate 6 cycles of modulation of the amplified MRMFT trace (MRMFT, 100×; AC) related to the cardiac cycle. (B) Recording showing individual action potentials and MFT recording. Upper scale bar = 10°; lower scale bar = 220 mg (MRMFT) and 4.4 mg (MRMFT, 100×; AC). Abbreviations: HL – horizontal left eye position; HR – horizontal right eye position; MRMN – medial rectus motoneuron spike train.

3. Results

We recorded from 33 medial rectus motoneurons in 3 animals. An example of an 18-s trial is shown in Fig. 2A. The DC-coupled signal from the strain gauge amplifier accurately reflects changes in medial rectus muscle force during horizontal eye movements (Fig. 2A; MRMFT signal).

We found that animals can stably fixate at eccentricities associated with motoneuron firing rates of 10–30 spikes/s for long enough to collect stable, amplified MFT samples (Fig. 2A; MRMFT, 100×; AC signal), despite their brief saturation immediately following a saccade. We observed that the baseline of the AC-coupled, amplified MFT signal was slightly modulated by the cardiac cycle (Fig. 2A; MRMFT, 100×; AC signal; six cycles indicated by arrows), and that this artifact was stronger in some eye positions than others. The frequency of this modulation (~2–3 Hz) was sufficiently low that it did not interfere with higher-frequency twitch activity (Fig. 2B; MRMFT, 100×; AC signal), and being uncorrelated with motoneuron firing, added only slight noise to our data.

We applied STA-MFT analysis to all recorded motoneurons, and obtained significant twitch measurements for 20 motoneurons. An example of a twitch for a medial rectus motor unit is shown in Fig. 3A.

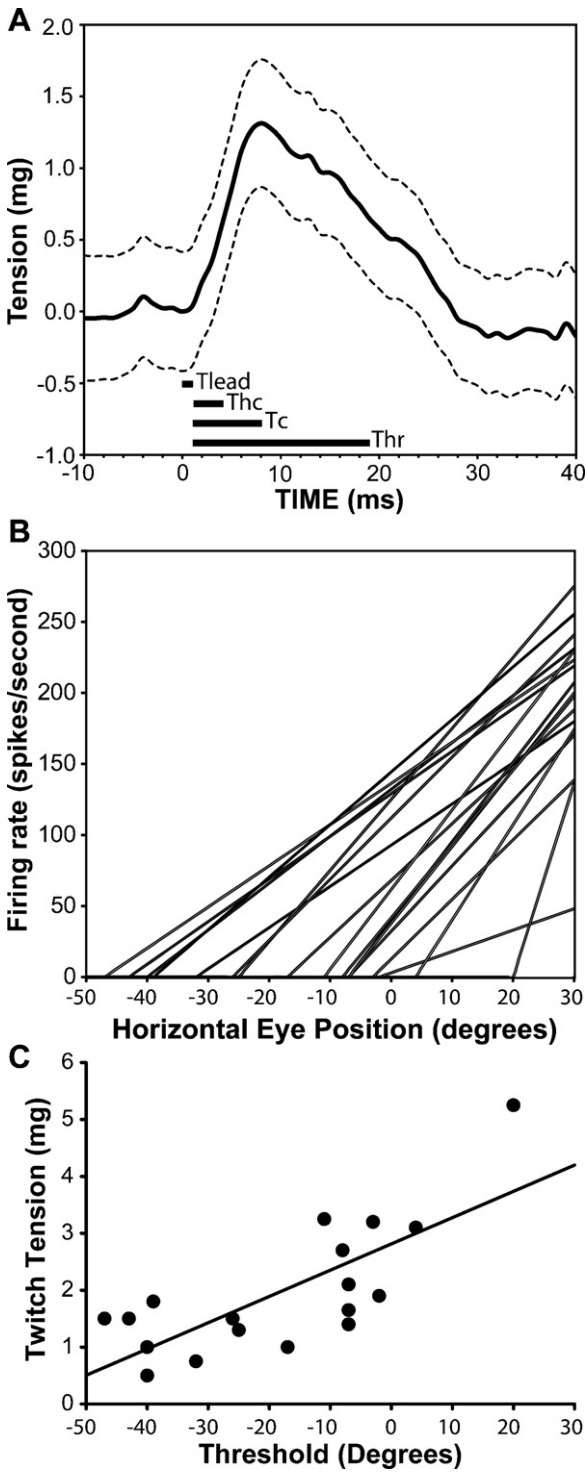

Fig. 3. (A) Spike-triggered average from the medial rectus motor unit shown in Fig. 2. Dotted lines are 95% confidence limits, mean interspike interval ~33 ms, and number of spikes used to generate the average = 3934. Abbreviations: Tlead – initial twitch delay; Thc – time to half contraction; Tc – time to peak contraction; Thr – time to half relaxation. (B) Plot showing the firing rate changes of the motoneurons in this study for changes in eye position brought about by conjugate eye movements. (C) The relationship between motor unit twitch tension and recruitment threshold. Medial rectus muscle motor units are recruited such that stronger motor units reach threshold further in the muscle's ON-direction ($R^2 = 0.57$).

Overall, for 20 medial rectus motor units, we measured twitch tensions of 0.5–5.25 mg (mean = 2.0 mg; SD = 1.2 mg). These motor units displayed an initial twitch delay (Tlead) of 1–4 ms (mean = 2.4; SD = 0.7 ms). Time to half contraction (Thc) varied from 3.0 to 8.5 ms (mean = 4.2 ms; SD = 1.3 ms); time to peak contraction (Tc) varied from 6 to 15 ms (mean = 9.3 ms; SD = 3.5 ms); time to half relaxation (Thr) varied from 10 to 32 ms (mean = 20.5ms; SD = 7.1 ms). We were unable to extract twitches for the 13 other motoneurons because: (1) an insufficient number of spikes (<1000) were available to obtain significant spike-triggered averages (5 motoneurons); (2) single-unit isolation for the duration of testing was inadequate (3 motoneurons); (3) average firing rates often exceeded 50 spikes/s (2 motoneurons); (4) no significant twitch could be extracted despite having a large number of spikes at low firing rates with good isolation (3 motoneurons). Of the 20 medial rectus motor units from which we extracted twitch responses, we were able to characterize 18 with respect to their recruitment threshold and their activity for changes in eye position brought about by saccadic eye movements (Fig. 3B), and the relationship of twitch magnitude to recruitment threshold. We found that these motor units are recruited in order of twitch tension magnitude with stronger motor units reaching threshold further in the muscle's ON-direction (Fig. 3C).

4. Discussion

We have shown that it is possible to extract individual extraocular muscle twitches using motoneuron spike-triggered averaging of MFT signals (STA-MFT) in alert macaques. The twitches we measured have temporal characteristics consistent with those reported for anesthetized squirrel monkey (Goldberg et al., 1998), and whole-nerve stimulation of the abducens nerve in alert monkeys (e.g. Fuchs and Luschei, 1971). In addition, the measured twitch forces are consistent both with data from the inferior rectus of unanesthetized rabbits (Barmack, 1977), and with the value predicted by dividing whole-nerve twitch tension (~4 g) (Fuchs and Luschei, 1971) by estimated medial rectus motoneuron number (~2000) (Spencer and Porter, 1988).

The twitch forces reported for alert macaque monkey with the STA-MFT technique are substantially smaller in amplitude than those reported in anesthetized squirrel monkey (Goldberg et al., 1998), suggesting that "sub-summation" (total muscle force being less than estimated summed twitches across all motor units) is not as dramatic as reported by Golderg and colleagues. Sub-summation might have been observed in their study because lateral rectus muscle length was adjusted (possibly beyond the normal physiological range) so as to produce the largest isometric twitch tension when the abducens nerve was stimulated (Goldberg et al., 1998). The suggestion that motor unit forces sum in a relatively linear fashion would be consistent with the observation that most myofibers in the orbital layer of the macaque medial rectus muscle extend from tendon to tendon and, although some myofibers in the global layer leave one fascicle to join a nearby fascicle, most fibers remain in defined fascicles that can be traced anteriorly to the tendon (Lim et al., 2007). In addition, few (~5%) myomyous junctions are seen in macaque or rabbit rectus muscles and these are primarily close to the muscle origin (Davidowitz et al., 1977; Lim et al., 2007). However, a number of other studies have reported that myofibers in both the orbital and global layers of the mammalian extraocular muscle are significantly shorter than the muscle length and that branching and serial connections between the fibers are prevalent (e.g. McLoon et al., 1999; Harrison et al., 2007). If this is the case and if, as we suggest, motor unit forces in extraocular muscle sum in a relatively linear fashion, it will be important to understand how the innervation of extraocular muscle myofibers by individual motoneurons is organized in order to produce this outcome.

4.1. Not all motor units produce measurable twitches

We could not extract twitch signals from 13 of our sample of 33 MNs (39%), and in 3 (9%) no twitch was evident despite having a large number of spikes at low firing rates with good isolation. This result is not surprising since one would not expect all motor units to yield twitches that are evident at the tendon. First, some motor units appear to serve a regulatory function, rather than contributing directly to oculorotary force (Buttner-Ennever and Horn, 2002), in which case we might measure no correlated force change at the tendon. A different sort of regulatory function is served by orbital layer fibers inserting in extraocular muscle pulley tissues (Miller, 1989, 2007; Demer et al., 2000), which anatomic studies make clear couple to the eye only indirectly (Oh et al., 2001), and might therefore produce little oculorotary force. Second, a motoneuron that innervates non-twitch, multiply-innervated fibers, such as are found in both orbital and global layers, would produce force changes that, regardless of their oculorotary effectiveness, would be too small and slow to be extracted with the current technique.

4.2. Motor unit recruitment

Our results indicate that medial rectus muscle motor units are recruited according to the size principle such that stronger extraocular muscle motor units reach threshold further in the muscle's on-direction (Henneman, 1957; Henneman et al., 1965). Thus, the eye movement system appears to behave like other skeletal systems, recruiting weak motor units to produce fine gradations at low force levels, and strong units to produce substantial increments at high force levels (Milner-Brown et al., 1973; Bagust et al., 1973; Burke et al., 1973; Llewellyn et al., 2010). This is a significant finding, since, in the absence of motor unit data from alert animals, previous modeling had suggested a *U*-shaped recruitment order for extraocular muscle motor units, with strong units recruited initially, weaker units next, and then stronger units closer to primary position (Dean, 1996).

4.3. Motor unit characterization vs. motor unit participation

The STA-MFT technique requires that the firing rate of the triggering motoneuron be low enough (10–30 Hz in the present study) that muscle twitches do not follow each other too closely since, because of the regularity of oculomotor firing, they would then partially summate. Overlap results in underestimation of twitch force because it causes overestimation of the force baseline, and would result in underestimation of contraction time if one took a twitch to be finished when it was only obscured by a subsequent twitch (e.g. Taylor et al., 2002). That is, the STA-MFT technique inherently requires firing rates low enough for underlying twitches to be distinguished. Thus, we could not characterize 2 (6%) of our units because we could not obtain stable firing at sufficiently low rates. It would therefore be worthwhile to develop methods for extending the range of firing rates for which twitches can be extracted, and we believe that modest twitch overlap could be accommodated using model-based deconvolution (e.g. Raikova et al., 2007, 2010). It may even be possible to extend the STA-MFT technique to extract responses from multiply innervated non-twitch motor units (Buttner-Ennever et al., 2001).

However, it is important to appreciate that there is no relationship between the low firing rates needed for MFT-STA twitch extraction and characterization, and the high and/or rapidly varying firing rates that might be associated with the participation of a motor unit in gaze holding at a particular orbital position or in a rapid eye movement such as a saccade. In the present study, for example, we used low firing rates to characterize motor units having twitch amplitudes that varied over a 10-fold range, and

were then able to determine the participation of each – its position threshold and saccadic response – at much higher firing rates.

4.4. Limitations of the STA-MFT technique

One limitation of the current technique is that each motor unit is characterized with the eye at a particular gaze position. Therefore, systematic differences in the length and active tension of the muscle might be expected to affect the amplitude and possibly time course of the measured twitch. In cat peroneus longus muscle, single twitch contractions of slow and some fast fatigue-resistant motor units linearly increase with muscle length while single twitch contractions of other fast motor units, both fatiguable and fatigue-resistant, display a "classic" length–tension curve with peak tension generated at an intermediate muscle length and reduced tension at shorter and longer lengths (Filippi and Troiani, 1994). These potential influences of muscle length and active tension on the amplitude and duration of measured twitches could be studied using STA-MFT while the muscle length is varied systematically by application of external forces to the eye (e.g. Keller and Robinson, 1971) as well as for single twitch contractions elicited at different eye positions by motoneuron axon microstimulation (e.g. Westling et al., 1990; Thomas et al., 1990; Thomas, 1995; Macefield et al., 1996).

Spike-triggered averaging of muscle force signals has been shown by simulation to require careful interpretation (Taylor et al., 2002). Multi-unit synchronization is a potential problem in all STA studies because averaging removes only uncorrelated activity, and if activity of other motor units were correlated with the triggering MN, measured twitch force would be artifactually increased, twitch duration increased, and the twitch profile distorted. We do not think this is a significant problem for STA-MFT. First, from the size principle, eye positions that yield the low firing rates used for characterization of a particular motor unit also leave more powerful motor units below threshold, and so, unable to interfere. Second, in a study of lateral rectus motoneurons that included EMG measurements, Fuchs et al. (1988) found limited motoneuron synchronization.

A practical complication in the STA-MFT technique is that an eye-position dependent cardiac pulse causes baseline modulation even during steady fixation (see Fig. 2A and B). This increases the variability of MFT signals, increasing the number of samples needed for twitch extraction. Cardiac-related STA artifacts have been observed in another study of extraocular muscle in macaques (Quaia et al., 2009) and in a study of extensor digitorum brevis twitches in humans (Macefield et al., 1996). In the macaque study, the artifact was removed using a template approach, while in the human study the electrocardiogram (ECG) signal was used to gate data collection. In future studies, these approaches could be used to remove cardiac-related artifacts from the recorded MFT signals.

5. Future studies

The STA-MFT technique should also be useful in studying other motor unit properties. For example, based on histological appearance and immunohistochemical properties, global layer fast-twitch fibers are thought to differ in fatigue resistance, and that this difference is related to recruitment order (Porter et al., 1995). Fatigue in skeletal muscle fibers is known to occur mainly in excitation–contraction coupling, and typically results in slowed twitch rise times, prolonged decays, and reduced forces (Bigland-Ritchie and Woods, 1984). The STA-MFT technique could be used to test these notions with direct measurements of motor unit fatigue.

Acknowledgements

Supported by National Institutes of Health, National Eye Institute grants EY015314 to JMM and P30 EY03039 to UAB. Kristen Sandefer, Julie Hill, Danielle Alexander, Sam Hayley, Corey Penn, Kevin Shieh, Debbie Whitten, Abi Yildirim, and Jerry Millican provided technical assistance. Dr. Ryan Davison helped with initial data collection.

Appendix A.

A.1. MFT fabrication, testing and implantation

The MFT/M-2.11 muscle force transducer for monkey extraocular muscle is described below in sufficient detail to understand how it is made and used. Detailed fabrication instructions are available at www.eidactics.com/Eidactics-branch/Products/MFT/MFT-Fabrication.pdf.

A.2. Frame

Our muscle force transducer for monkey extraocular muscle, MFT/M-2.11, is fabricated from 10-mil half-hard stainless steel sheet. Blank frames are cut by photochemical etching (Elcon Co., San Jose, CA), electro-polished, and manually finished to remove sharp edges that might damage muscle or tendon. Half-depth engravings on the top of the frame define lines along which the four "ears" are bent upward at right angles to form bearings for an Attachment Pin that directs the muscle through the frame. The side of the frame without bearings or wiring (Fig. 1, top) contains tie-down holes used to maintain MFT orientation during healing, and is bent down 20° so the device better conforms to the globe, preventing the muscle from losing any of its 3 lines of contact with the device when wrapped around the globe. Bearing holes are sized to fit the 26 ga Attachment Pin after Parylene coating. To improve strain gauge bonding and coating adhesion, frames are sandblasted and cleaned with acetone (Fig. A.1).

A.3. Gauging and wiring

Transducer-grade, *U*-shaped, semiconductor strain gauges were chosen for their small size and high gauge factor (sensitivity to

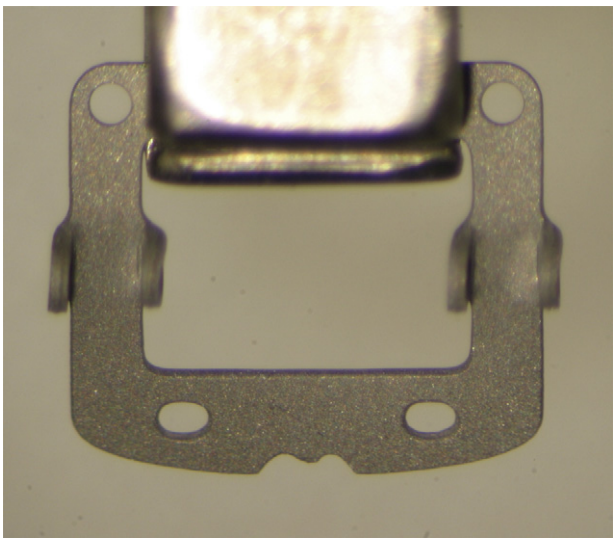

Fig. A.1. Finished frame, held in custom forceps, also used for implantation. Wiring passes from bottom to top of frame through oblong holes at bottom. Attachment Pin (not shown) passes through upward-bent ears and under muscle at middle. Tie-down holes at top secure device to muscle margins to stabilize orientation during healing.

strain). One gauge is bonded to the top surface of the frame and another to the opposite beam on the bottom. The two function differentially, with muscle tension compressing the top and elongating the bottom gauge. Wired as arms of a Wheatstone Bridge, this arrangement achieves high output, temperature compensation, and sums forces across the width of the muscle. Forty-gauge copper "magnet" wire joins one side of each gauge. This common wire, and the two free gauge wires are connected, via solderable connection pads, to Teflon insulated stainless-steel multi-stranded lead wires (AS-631, Cooner Wire, www.coonerwire.com), such that, to lengthen paths of possible leakage, the points of attachment are as far as possible from where the lead wires depart the encapsulated frame.

Mounting surfaces are etched and neutralized (M-Prep Conditioner A & M-Prep Neutralizer 5A, Vishay Micro-Measurements, www.micro-measurements.com), and a fine brush is used to apply two thin insulating base coats of M-Bond 610 epoxy adhesive (Vishay) under the areas that will receive strain gauges, connection pads and lead wires. Solder connection terminals are shaped from MST-035 and MST-094 bondable terminals (Micron Instruments, www.microninstruments.com) to be as small as possible to minimize surfaces over which electrical leaks might develop, tinned with 430 °F solder, and grooved to position the fragile gold strain gauge lead wires. Entran ESU-025-500-4 semiconductor strain gauges (www.meas-spec.com) are used in matched sets. After cleaning a strain gauge and a set of prepared terminals in acetone to remove any contaminants that might impair bonding, we brush a layer of M-Bond 610 on the bonding surfaces of the frame and position the strain gauge, making certain that a small fillet of epoxy forms around it. Unlike film gauges, silicon gauges shatter if clamped, so it is critical to apply enough epoxy to form a complete bond, but no so much as to float the gauge above the frame, which would result in compliant mechanical coupling. We position the terminals on the wet epoxy, air-dry in a dust-free chamber overnight, and then bake for 2 h at 165 °C. We then gently lay the strain gauge's gold lead wires into their terminal grooves, and cut them to size. We repeat the process on the other side of the frame.

The 50 ga gold strain gauge wires tend to dissolve in molten solder. We apply acid flux with a sharpened toothpick, and working quickly, solder the gold wires to their terminals using a miniature screwdriver-shaped tip (Weller MT221) on a temperature-controlled 410 °F iron carrying a small amount of 316 °F solder, clean the joint of flux, and neutralize residual acid. We then join the near sides of the top and bottom strain gauges via their terminals with magnet wire passing through one of the frame's oblong holes (see Fig. A.1).

We condition the proximal ends of the FEP-insulated stainless steel lead wires with Tetra-Etch adhesion promoter (Gore, Newark, DE), wash in warm water followed by acetone, strip, tin with 430 °F solder, clean, and neutralize. We position wires for soldering with a manipulator incorporating an E-Z-Micro-Hook X2015, attached to a photographer's "Israeli Arm", mounted on a weighted base. Lead wires are soldered to their connectors with the 410 °F iron and 316 °F solder. Two lead wires pass up through the oblong hole along with the copper interconnect wire, join the lead wire soldered to the connector on the free end of the top strain gauge, and the 3 wires are braided. A silicone rubber strain-relief sleeve (2.0 mm long × 0.025in OD × 0.012 in ID), prepared with Tetra-Etch, is slipped up the lead wires, onto the frame, and tied to the frame with 6-0 Prolene suture.

A.4. Encapsulation

MFTs are encapsulated in Parylene-C, up to but not including the FEP-insulated lead wires, to provide a biocompatible moisture barrier for strain gauges, on-board wiring, and the frame itself.

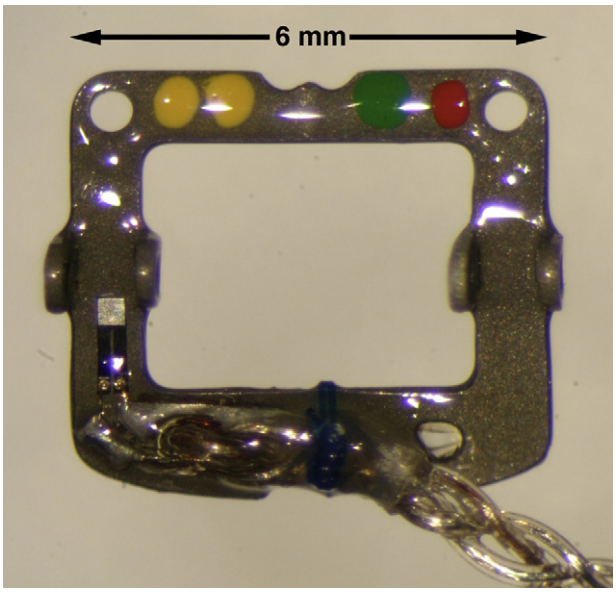

Fig. A.2. MFT. A stainless steel frame carries two semiconductor strain gauges (one visible at the lower left, the other on the underside of the opposite beam, at the lower right), wired as a half Wheatstone Bridge, and positioned to average forces across the tendon and compensate for variations in temperature. The device is encapsulated in epoxy resin and Parylene-C. It is affixed by pushing a pin (not shown) through holes in the 4 upward-bent tabs, and under the muscle. Devices are fabricated in 2 orientations: "left" (shown), for implantation on left LR and right MR, and "right", for right LR and left MR, the intent being that posteriorly oriented lead wires course superiorly in the orbit as they depart the device.

The strain-relief assembly and surface wiring must first be fixed in place, and the strain gauges and their gold lead wires mechanically protected. Sharp protrusions must also be buried to prevent Parylene covering such spots from being selectively abraded during implantation.

We clean the devices in alcohol and coat them with Resin-Lab EP-1121 Clear Epoxy Encapsulant (Ellsworth Adhesives, www.ellsworth.com), except for the lead wires and the part of the frame that will be held in MFT Forceps during implantation, which must be protected from the pressure of the forceps with harder epoxy. Mixed but uncured, EP-1121 has very low viscosity, allowing it to wick into small gaps. Cured by baking at 65 °C for 2 h, it becomes tough but compliant, and can be applied as needed without affecting device sensitivity. Terminals, strain gauges and wiring are given several coats, and the strain-relief sleeve is filled, sealing the FEP-coated lead wires against the silicone rubber sleeve. The distal side of the frame is then serialized with colored enamel paint dots, baked, coated with hard (Vishay AE-15) epoxy, and baked again. A final coating of EP-1121 is applied to bridge the areas of hard and soft epoxy (Fig. A.2).

Lead wires are masked with silicone rubber sleeves, open at their ends to allow air exchange, but long enough to prevent Parylene vapor intrusion. Devices are cleaned, and etched with cold plasma to improve adhesion. Parylene-C is then vapor-deposited to a thickness of 20 μm (Plasma Ruggedized Solutions, San Jose, CA).

A.5. Testing and calibration

We measure and record resistance of each strain gauge at several points during fabrication. To test the integrity of encapsulation, we suspend each MFT in warm, stirred saline for several weeks, periodically testing for leaks between grouped lead wires and bath with a Fluke 189 Multimeter, which can detect leakage resistances greater than 500 MΩ. If a leak is found, we localize it by immersing

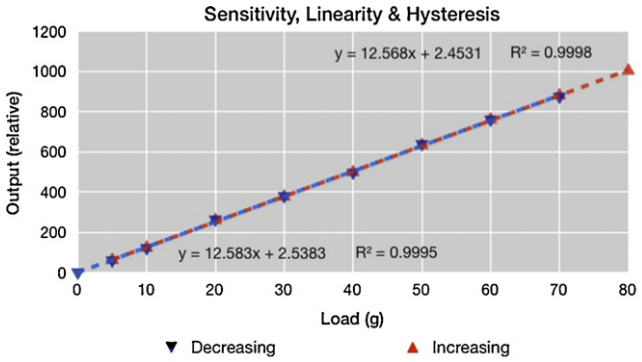

Fig. A.3. Typical MFT calibration. Graph showing output as a function of load during loading and unloading. Note the high sensitivity and linearity and absence of hysteresis.

the MFT in saline, connecting it to a cathode, the bath to an anode, and applying up to several hundred volts. At the cathode, H_2 is liberated from H_2O, and Na from NaCl. The liberated sodium pulls OH^- ions from H_2O, liberating more H_2. H_2 bubbles thus appear where the bath contacts electrically exposed components. Repair is sometimes possible, though this test has been more useful in refining design and fabrication.

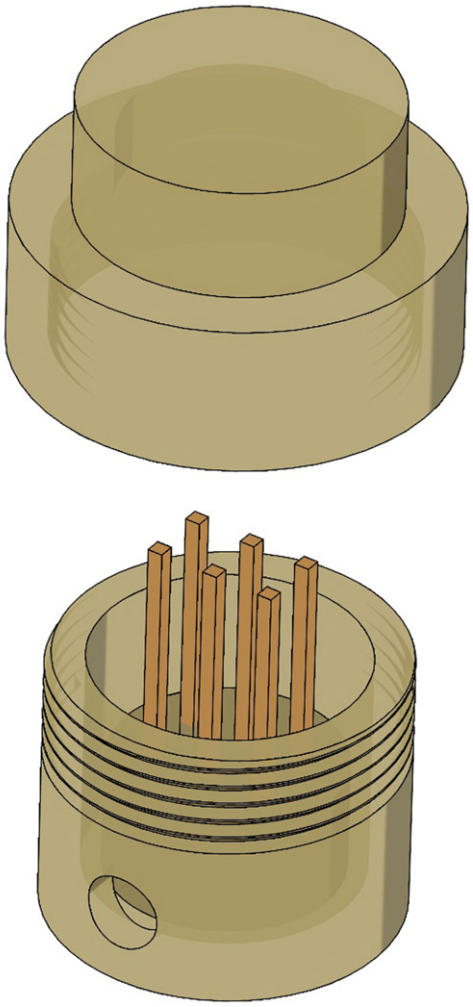

Fig. A.4. MFT Connector Can is fabricated from PEEK plastic and fitted with gold-plated IC pins with standard 0.1 inch spacing. Leads from 2 MFTs can be accommodated. The leads enter the hole near the bottom, which is then sealed with RTV silicone, wrap around the internal pedestal, and are soldered to connector pins near their bottoms. Standard connectors plug into the free ends of the pins. A screw cap protects the pins when not in use.

Each MFT is calibrated by attaching it to an strain gauge amplifier with 2 V excitation, inserting an Attachment Pin through its bearings, threading a length of 1/8″ wide Mylar tape through it as the muscle would go, and hanging weights 5–80 g from the end of the tape in ascending and descending series. All functioning devices have similar sensitivities, and are almost perfectly linear (Fig. A.3).

A.6. Implantation

MFTs have been chronically implanted in monkeys on lateral and medial recti. Under general anesthesia, with body supine, we spread the lids with a speculum or traction sutures, and disinsert the conjunctiva at the limbus in quadrants containing muscles to be implanted, placing traction sutures in cut edges of the conjunctiva to aid in visualizing the muscle. We clear the muscle of attachments by blunt dissection to about 10 mm posterior to the limbus, slide a standard ophthalmic muscle hook under it, and then transfer the muscle to an MFT Tendon Lifter (Fig. 1A and B).

Holding an MFT in its Forceps, we pass the Tendon Lifter and muscle up through the MFT's aperture. Pulling the muscle gently up, while holding the MFT down, we push an "Attachment Pin" through the proximal bearings, under the muscle, and through the distal bearings. With the MFT positioned a few mm behind the insertion, and oriented squarely on the muscle, we pass a 6-0 Prolene suture with a round, non-cutting needle through each tie-down hole and tie it to the underlying muscle margin. It is essential to stabilize the MFT until it becomes enveloped in connective tissue. We then position the lead wire in the orbit, allowing some slack, and route it to the scalp, following the method used to implant eye coil wires (Judge et al., 1980).

Because strain gauge signals are, essentially, small resistance changes, electrical connections must be scrupulously clean. We pass the braided MFT lead wires, uninterrupted, into a special plastic "Connector Can", where they are soldered to easily cleaned pins, onto which strain gauge amplifier connections are made (Figs. 1C and A.4). A successfully implanted device is stable for several months or longer.

References

Alvarado JA, Van Horn C. Muscle cell types of the cat inferior oblique. In: Lennerstrand G, Bach-y-Rita P, editors. Basic mechanisms of ocular motility and their clinical implications. Oxford: Pergamon; 1975. p. 15–43.
Bagust J, Knott S, Lewis DM, Luck JC, Westerman RA. Isometric contractions of motor units in a fast twitch muscle of the cat. J Physiol (Lond) 1973;231:87–104.
Barmack NH. Recruitment and suprathreshold frequency modulation of single extraocular muscle fibers in the rabbit. J Neurophysiol 1977;40:779–90.
Bigland-Ritchie B, Woods JJ. Changes in muscle contractile properties and neural control during human muscular fatigue. Muscle Nerve 1984;7:691–9.
Burke RE, Levine DN, Tsairis P, Zajac III FE. Physiological types and histochemical profiles in motor units of the cat gastrocnemius. J Physiol (Lond) 1973;234:723–48.
Buttner-Ennever JA, Horn AKE, Scherberger H, D'Ascanio P. Motoneurons of twitch and nontwitch extraocular muscle fibers in the abducens, trochlear, and oculomotor nuclei of monkeys. J Comp Neurol 2001;438:318–35.
Buttner-Ennever JA, Horn AKE. The neuroanatomical basis of oculomotor disorders: the dual motor control of extraocular muscles and its possible role in proprioception. Curr Opin Neurol 2002;15:35–43.
Cheney PD. Response of rubromotoneuronal cells identified by spike-triggered averaging of EMG activity in awake monkeys. Neurosci Lett 1980;17:137–41.
Davidowitz J, Philips G, Breinin GM. Organization of the orbital surface layer in rabbit superior rectus. Invest Ophthalmal Vis Sci 1977;16:711–29.
Dean P. Motor unit recruitment in a distributed model of extraocular muscle. J Neurophysiol 1996;76:727–42.
Demer JL, Oh SY, Poukens V. Evidence for active control of rectus extraocular muscle pulleys. Invest Ophthalmol Vis Sci 2000;41:1280–90.
Filippi GM, Troiani D. Relations among motor unit types, generated forces and muscle length in single motor units of anaesthetized cat peroneus longus muscle. Exp Brain Res 1994;101:406–14.
Fuchs AF, Luschei ES. Development of isometric tension in simian extraocular muscle. J Physiol 1971;219:155–66.

Fuchs AF, Scudder CA, Kaneko CRS. Discharge patterns and recruitment order of identified motoneurons and internuclear neurons in the monkey abducens nucleus. J Neurophysiol 1988;60:1874–95.
Gamlin PDR, Gnadt JW, Mays LE. Abducens internuclear neurons carry an inappropriate signal for ocular convergence. J Neurophysiol 1989;62:70–81.
Gamlin PDR, Mays LE. Dynamic properties of medial rectus motoneurons during vergence eye movements. J Neurophysiol 1992;67:64–74.
Gamlin PD, Yoon K. An area for vergence eye movement in primate frontal cortex. Nature 2000;407:1003–7.
Goldberg SJ, Meredith MA, Shall MS. Extraocular motor unit and whole-muscle responses in the lateral rectus muscle of the squirrel monkey. J Neurosci 1998;18:10629–39.
Goldberg SJ, Shall MS. Motor units of extraocular muscles: recent findings. Prog Brain Res 1999;123:221–32.
Harrison AR, Anderson BC, Thompson LV, McLoon LK. Myofiber length and three-dimensional localization of NMJs in normal and botulinum toxin treated adult extraocular muscles. Invest Ophthalmol Vis Sci 2007;48(8):3594–601.
Henneman E. Relation between size of neurons and their susceptibility to discharge. Science 1957;126:1345–7.
Henneman E, Somjen G, Carpenter. DO functional significance of cell size in spinal motoneurons. J Neurophysiol 1965;28:560–80.
Judge SJ, Richmond BJ, Chu FC. Implantation of magnetic search coils for measurement of eye position: an improved method. Vision Res 1980;20:535–8.
Keller EL, Robinson DA. The absence of stretch reflex in extraocular muscles of the monkey. J Neurophysiol 1971;34:908–19.
Lemon RN. Cortical control of the primate hand. Exp Physiol 1993;193:263–301 (The Brown GL Prize Lecture).
Lim KH, Poukens V, Demer JL. Fascicular specialization in human and monkey rectus muscles: evidence for anatomic independence of global and orbital layers. Invest Ophthalmol Vis Sci 2007;48:3089–97.
Llewellyn ME, Thompson KR, Deisseroth K, Delp SL. Orderly recruitment of motor units under optical control in vivo. Nat Med 2010;16:1161–5.
Macefield VG, Fuglevand AJ, Bigland-Ritchie B. Contractile properties of single motor units in human toe extensors assessed by intraneural motor axon stimulation. J Neurophysiol 1996;75:2509–19.
McLoon LK, Rios L, Wirtschafter JD. Complex three-dimensional patterns of myosin isoform expression: differences between and within specific extraocular muscles. J Muscle Res Cell Motil 1999;20(November (8)):771–83.
Miller JM. Understanding and misunderstanding extraocular muscle pulleys. J Vision 2007;7:1–15.
Miller JM. Functional anatomy of normal human rectus muscles. Vision Res 1989;29:223–40.
Miller JM, Robins D. Extraocular-muscle forces in alert monkey. Vision Res 1992;32:1099–113.
Miller JM, Bockisch CJ, Pavlovski DS. Missing lateral rectus force and absence of medial rectus co-contraction in ocular convergence. J Neurophysiol 2002;87:2421–33.
Miller JM, Davision RC, Gamlin PD. Motor nucleus activity fails to predict extraocular muscle forces in ocular convergence. J Neurophysiol 2011;105:2863–73.
Milner-Brown HS, Stein RB, Yemm R. The orderly recruitment of human motor units during voluntary isometric contractions. J Physiol (Lond) 1973;230:359–70.
O'Donovan MJ, Hoffer JA, Loeb GE. Physiological characterization of motor unit properties in intact cats. J Neurosci Methods 1983;7:137–49.
Oh SY, Poukens V, Demer JL. Quantitative analysis of rectus extraocular muscle layers in monkey and humans. Invest Ophthalmol Vis Sci 2001;42:10–6.
Peachey LD, Takeichi M, Nag AC. Muscle fiber types and innervation in adult cat extraocular muscles. In: Milhorat AJ, editor. Exploratory concepts in muscular dystrophy. New York: Elsevier; 1974. p. 246–54.
Porter JD, Baker RS, Ragusa RJ, Brueckner JK. Extraocular-muscles – basic and clinical sspects of structure and function. Surv Ophthalmol 1995;39:451–84.
Quaia C, Ying HS, Nichols AM, Optican LM. The viscoelastic properties of passive eye muscle in primates. I. Static forces and step responses. PLoS One 2009;4(4):e4850.
Raikova R, Celichowski J, Pogrzebna M, Aladjov H, Krutki P. Modeling of summation of individual twitches into unfused tetanus for various types of rat motor units. J Electromyogr Kinesiol 2007;17:121–30.
Raikova R, Rusev R, Drzymała-Celichowska H, Krutki P, Aladjov H, Celichowski J. Experimentally verified mathematical approach for the prediction of force developed by motor units at variable frequency stimulation patterns. J Biomech 2010;43:1546–52.
Robinson DA. A method of measuring eye movement using a scleral search coil in a magnetic field. IEEE Trans Biomed Electron 1963;10:137–45.
Robinson DA. Oculomotor unit behavior in the monkey. J Neurophysiol 1970;33:393–403.
Shall MS, Goldberg SJ. Extraocular motor units – type classification and motoneuron stimulation frequency–muscle unit force relationships. Brain Res 1992;587:291–300.
Spencer RF, Porter JD. Structural organization of the extraocular muscles. In: Buttner-Ennever JA, editor. Neuroanatomy of the oculomotor system. Amsterdam: Elsevier; 1988. p. 33–79.
Sylvestre PA, Cullen KE. Quantitative analysis of abducens neuron discharge dynamics during saccadic and slow eye movements. J Neurophysiol 1999;82:2612–32.
Taylor AM, Steege JW, Enoka RM. Motor-unit synchronization alters spike-triggered average force in simulated contractions. J Neurophysiol 2002;88:265–76.
Thomas CK, Ross BH, Stein RB. Motor-unit recruitment in human first dorsal interosseous muscle for static contractions in three different directions. J Neurophysiol 1986;55:1017–29.
Thomas CK, Bigland-Ritchie B, Westling G, Johansson RS. A comparison of human thenar motor-unit properties studied by intraneural motor-axon stimulation and spike-triggered averaging. J Neurophysiol 1990;64(October (4)):1347–51.
Thomas CK. Human motor units studied by spike-triggered averaging and intraneural motor axon stimulation. Adv Exp Med Biol 1995;384:147–60.
Walmsley B, Hodgson JA, Burke RE. The forces produced by medial gastrocnemius and soleus muscles during locomotion in freely moving cats. J Neurophysiol 1978;41:1203–16.
Westling G, Johansson RS, Thomas CK, Bigland-Ritchie B. Measurement of contractile and electrical properties of single human thenar motor units in response to intraneural motor-axon stimulation. J Neurophysiol 1990;64(October (4)): 1331–8.
Zhang H, Gamlin PD. Neurons in the posterior interposed nucleus of the cerebellum related to vergence and accommodation. I. Steady-state characteristics. J Neurophysiol 1998;79:1255–69.